

Adaptive Electromagnetic Vibration Absorber for a Multimode Structure

Khaled S. Mohamed¹ – Fatin Amri² – Mostafa Elborae¹ – N.H. Diyana Nordin² – Asan G.A. Muthalif^{1,*}

¹ Qatar University, College of Engineering, Qatar

² International Islamic University Malaysia, Department of Mechatronics Engineering, Malaysia

All structures experience vibrations due to external dynamic force excitations, such as earthquakes and wind loadings. At resonance, the impact of this natural dynamic force on structures may lead to structural failures. Hence, an absorber is mounted to absorb vibrations from the primary system. Unfortunately, passive tuned mass absorbers can only target a single frequency. Since structural buildings possess multiple modes, an adaptive or tune-able vibration absorber is needed to attenuate the vibration in a multi-degree of freedom (MDOF) system. In this work, an adaptive electromagnetic vibration absorber (AEMVA) is proposed to eliminate the effects of vibrations and is dynamically tuned using electromagnets. By varying the current supplied to the coil, the stiffness of the AEMVA can be adjusted, resulting in a varying absorber frequency. A mathematical description of the AEMVA on a three-story prototype model building is also presented. The three-story benchmark model was used to demonstrate the effectiveness of AEMVA in absorbing multiple vibration modes, both analytically and experimentally. It is shown that 68.81 %, 50.49 %, and 33.45 % of vibration amplitude reductions were achieved at the first, second, and third modes, respectively.

Keywords: adaptive vibration absorber, electromagnetic vibration absorber, multimode system, dynamic modelling, structural vibration control

Highlights

- A dynamic system AEMVA with a variable natural frequency was proposed to absorb the vibration of a multi-degree of freedom system.
- The basic theory and design for AEMVA were derived.
- Experimental analysis was carried out using a benchmark model of a three-story building.
- Tuning of the dynamic system proved successful in reducing the amplitude of the vibrations.

0 INTRODUCTION

Three decades ago, fewer skyscrapers existed. Due to limited spaces and resources, buildings are now often built with a higher number of levels. However, high-rise buildings are prone to vibrations, such as wind-induced vibrations, causing excessive deflections and massive failures. Since high-rise buildings possess multiple modes of natural frequency, a tuneable-dynamic vibration absorber should be opted to eliminate unwanted vibrations.

In suppressing structural vibrations, passive control devices utilizing liquid or solid masses are widely studied. Lumped masses were used for bridge piers with improved efficiency of 25 % [1], liquid column-based dampers were used for structural control with effective results [2], and new damping methods were introduced for closely spaced natural frequencies for an enhanced accuracy damping technique [3]. Liquid-based dampers were introduced for controlling seismic vibrations for short-period structures [4], while wind-induced vibrations were also analysed for control in flexible structures [5]. The required damping level is tuned by adjusting the mass

of the liquid or solid based on the external excitations. Some devices were studied and designed for vibration suppression through variations of stiffness. Shape memory helical springs [6] were studied and enhanced for super-elastic shape memory helical springs [7], which were enhanced further to temperature-adjusted shape memory helical springs [8], and alloy pounding controlled dampers [9]. Magnetorheological elastomers [10] were also studied, and an attenuation controller was tested [11] for the practicality of the application, which was then enhanced to make use of conical magnetorheological elastomer isolators [12]. Gyro effects had been studied for a cantilever beam vibration isolation [13], and the technology was utilized in designing an intelligent glove for the suppression of Parkinson's disease effects [14], all of which were proven beneficial in controlling vibrations. Apart from being heavy [15], these types of absorbers work well only in narrow frequency bands [16]. Also, the system parameters might deteriorate due to wear, environmental, and operational conditions [17].

Magnetorheological fluids were introduced as a viable solution for the development of controllable dampers and were extensively used in many

*Corr. Author's Address: Department of Mechanical and Industrial Engineering, College of Engineering, Qatar University, Doha, Qatar, drasan@qu.edu.qa

applications for damping. In addition to having nonlinear hysteretic forces [18], recent studies show a maximum vibration reduction of 35 % to 37.2 % when the absorber is mounted on the first floor of a three-story building which was tested for a magnetorheological damper for earthquake-induced vibrations [19] and was enhanced to include neural networks [20], which were later enhanced further to include an intelligent bi-state controller [21], which proved beneficial but left room for improvements. Therefore, it is challenging to create high-efficiency magnetorheological (MR) fluid dampers that take advantage of the fluid features.

To overcome these issues, a vibration absorber capable of tuning its natural frequency in a wide frequency band, especially in a structure with multiple degrees of freedom, should be implemented. The force behaviour should be modelled and fully controlled with an understandable non-complex model to achieve high efficiencies exceeding the methods previously mentioned and be straightforward with fabrication.

In this work, the stiffness of the absorber is varied using electromagnetic coils. Variations in the current level applied to the magnetic coils directly influence the value of the generated magnetic field [17] and [22]. As a result, the damper’s stiffness changes accordingly, thus changing the absorber’s frequency

to match the multimode structure’s frequency. This allows for a damper that is suitably controlled for a wide frequency band.

1 ADAPTIVE VIBRATION ABSORBER USING ELECTROMAGNETS

A three-story building prototype model is used in this work; the floors were made of aluminium, and side support beams were made of stainless steel. Fig. 1 shows the prototype and schematic diagram, respectively. Stainless steel supporting columns are used, and equivalent stiffness for each floor can be modelled using Eqs. (1) and (2):

$$k_c = \frac{12EI}{L^3}, \tag{1}$$

$$I = \frac{bd^3}{12}, \tag{2}$$

where k_c is the stiffness for each column, and since we have four columns for each floor connected in parallel, the effective stiffness for each floor is equal to $4k_c$. I is the moment of inertia, E is the modulus of rigidity for stainless steel, b is the width for each column, d is the thickness of each column, and L is the length of each column. The stiffness around each floor

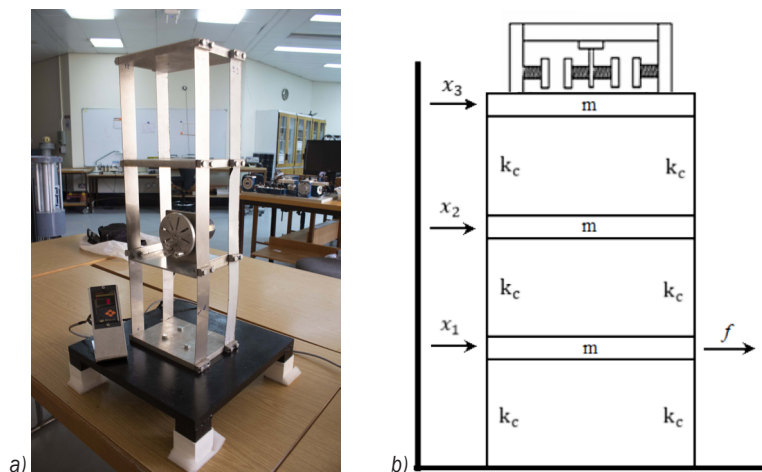


Fig. 1. a) 3-story building model, b) schematic of the absorber/3-story building

Table 1. Properties of building model

Floors (aluminium)		Columnal supports (Stainless steel)	
Length of each floor	200 mm	Length of each column	200 mm
Width of each floor	150 mm	Width of each column	40 mm
Thickness of each floor	15 mm	Thickness of each column	1 mm
Mass of each floor	1.50 kg	Modulus of elasticity	200 GPa
Density of aluminium	2.7×10^{-6} kg-mm ⁻³	Stiffness for each column	1 N/mm

is obtained using Eqs. (1) and (2), and the properties are given in Table 1.

The adaptive electromagnetic vibration absorber (AEMVA) mounted on top of the three-story building model studied in this work is shown in Fig. 1b. Four electromagnets and a prototype model of a three-story building Fig. 1b were used to study the efficiency of the AEMVA to absorb the vibration of the structure. The equation of motion for the structure can be represented in Eq. (3):

$$\mathbf{M}\ddot{\mathbf{x}} + \mathbf{C}\dot{\mathbf{x}} + \mathbf{K}\mathbf{x} = \mathbf{f}, \quad (3)$$

where \mathbf{M} is the mass matrix, \mathbf{C} is the damping matrix, \mathbf{K} is the stiffness matrix, and \mathbf{f} is the force function. For this project, any damping coefficients are neglected, and hence Eq. (4) summarizes the coefficients for Eq. (3).

$$\begin{bmatrix} m_1 & 0 & 0 & 0 \\ 0 & m_2 & 0 & 0 \\ 0 & 0 & m_3 & 0 \\ 0 & 0 & 0 & m_a \end{bmatrix} \begin{bmatrix} \ddot{x}_1 \\ \ddot{x}_2 \\ \ddot{x}_3 \\ \ddot{x}_a \end{bmatrix} + \begin{bmatrix} k_1 + k_2 & -k_2 & 0 & 0 \\ -k_2 & k_2 + k_3 & -k_3 & 0 \\ 0 & -k_3 & k_3 + k_a & -k_a \\ 0 & 0 & -k_a & k_a \end{bmatrix} \begin{bmatrix} x_1 \\ x_2 \\ x_3 \\ x_a \end{bmatrix} = \begin{bmatrix} f_1 \\ 0 \\ 0 \\ 0 \end{bmatrix}, \quad (4)$$

where \ddot{x} is the acceleration, and x is the horizontal displacement of the building. Subscripts 1, 2, and 3 represent the floor of the building, and subscript a refers to the absorber, making m_a the mass of the AEMVA absorber. In addition, m is the floor mass, and k denotes the stiffness. Each floor's mass and stiffness coefficients are as summarized in Table 1, while the absorber's mass m_a and stiffness coefficient k_a are to be examined in Section 3 for the proper tuning of the absorber.

2 ADAPTIVE ELECTROMAGNETIC VIBRATION ABSORBER MODELLING AND DESIGN

For the magnetic field at a point P with a distance D outside a ring of wire with radius R , the magnetic field from a small wire segment at the top of the ring can be modelled.

$$d\vec{\mathbf{B}} = \frac{\mu_0 I_{encl.}}{4\pi} \frac{d\vec{\mathbf{x}}}{D^2 + R^2} \frac{R}{\sqrt{D^2 + R^2}}. \quad (5)$$

Use Fig. 2 and Eq. (5) after accounting for the opposite vertical field directions. $I_{encl.}$ is the current supplied $I_{supp.}$ multiplied by the number of coils used.

By integrating the magnetic field over all the small segments of the coil $d\vec{\mathbf{x}}$, where the integration is the circumference of the circle, Eq. (6), the total field for a single loop at point P would arise [23].

$$\vec{\mathbf{B}}_{\text{single loop}} = \frac{\mu_0 I_{encl.}}{2} \frac{R^2}{(D^2 + R^2)^{3/2}}. \quad (6)$$

Eq. (6) represents the magnetic field strength for a single wire turn. For a solenoid integrating over all the coil turns is required, Fig. 2 is used.

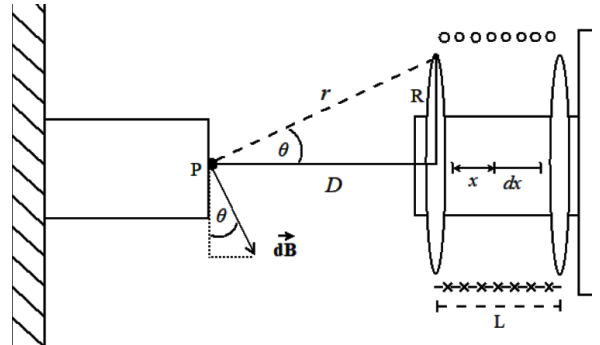


Fig. 2. Mathematical model representation for the damper

Rewriting Eq. (6) to include the previous findings gives Eqs. (7) and (8), where n is the number of coils per unit length of the solenoid.

$$I_{encl.} = I_{app.} n dx \quad (7)$$

$$\vec{\mathbf{B}}_{\text{total}} = \frac{\mu_0 I_{app.} n dx}{2} \frac{R^2}{((D+x)^2 + R^2)^{3/2}}, \quad (8)$$

integrating across the limits of x which is the length over the solenoid we obtain Eq. (9):

$$\vec{\mathbf{B}}_{\text{Total}} = \frac{\mu_0 I_{app.} n}{2} \times \left[\frac{D+L}{\sqrt{(D+L)^2 + R^2}} - \frac{D}{\sqrt{D^2 + R^2}} \right]. \quad (9)$$

For the force between the two nearby aligned electromagnets, we can use the Magnetic-Charge model to model the force from one magnet to the other as in Eq. (10):

$$F_{\text{repulsion}} = \frac{\vec{\mathbf{B}}_{\text{Total}} A}{2\mu_0}. \quad (10)$$

Modelling the electromagnets as a spring so forces can be modelled using Fig. 2 and Eq. (11):

$$F_{\text{repulsion}} = k_a \times D, \quad (11)$$

where D is the distance between the two electromagnets.

This gives Eq. (12) for the semi-spring constants:

$$k_a = \frac{A}{2\mu_0 \cdot \Delta x} \frac{\mu_{Carbon\ steel\ core} I_{app} \cdot n}{2} \times \left[\frac{D+L}{\sqrt{(D+L)^2 + R^2}} - \frac{D}{\sqrt{D^2 + R^2}} \right]. \quad (12)$$

We also have two springs connected to the mass in the middle, which means they are connected in parallel, and the equivalent stiffness we are looking for is $2k_a$ which gives Eq. (14) for all three vibration modes as follows, making use of Eq. (13) for the

natural frequency using the mass and the stiffness, and hence our unit for the natural frequencies is in radians per second:

$$\omega_n = \sqrt{\frac{k_{equivalent}}{m}}. \quad (13)$$

The final equation used for the natural frequencies of the system is Eq. (14); the physical parameters and properties of electromagnets are summarized in Table 2, and an iron core can be seen in Fig. 3a and b, which shows the full assembled absorber. The design was meant to maximize the repulsion force between two electromagnets of opposite polarity opposing each other.

$$\omega_n = \sqrt{\frac{\frac{A}{\mu_0 \cdot \Delta x} \frac{\mu_{Carbon\ steel\ core} I_{app} \cdot n}{2} \left[\frac{D+L}{\sqrt{(D+L)^2 + R^2}} - \frac{D}{\sqrt{D^2 + R^2}} \right]}{m_{absorber}}}. \quad (14)$$

Table 2. Electromagnets properties

Electromagnets (Carbon steel)			
Inner diameter	15 mm	Diameter of copper coil	5 mm
Outer diameter	30 mm	Number of coils	300
Length of core	24 mm	Mass of each core	150 g
Thickness of outer layer	4 mm	Range of current supplied	0 A to 3 A
Relative magnetic permeability	100		

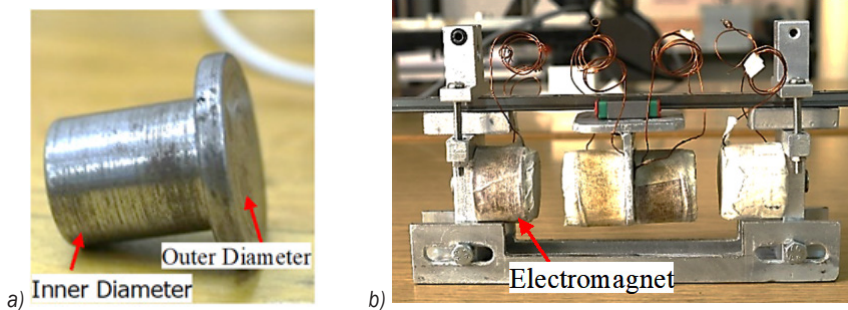


Fig. 3. a) Electromagnetic core, and b) AEMVA model

3 SIMULATION STUDIES OF ELECTROMAGNETIC VIBRATION ABSORBER (AEMVA)

Simulation studies were conducted for the system's response with and without the absorber. The parameters in the simulation studies are listed in Tables 1 and 2. Using Eq. (4), the natural frequencies of the three-story building are shown in Table 3.

An excitation input was applied to the building and based on Eq. (4), the response of the first floor at three modal frequencies was observed. Without an absorber, the displacement of the first floor is displayed in Fig. 4. Mode shapes at each nodal frequency are also shown in Fig. 5. Likewise, Fig. 6 shows the first floor's responses at three natural frequencies when the absorber is tuned to absorb each frequency. Frequencies are given in Hz, and

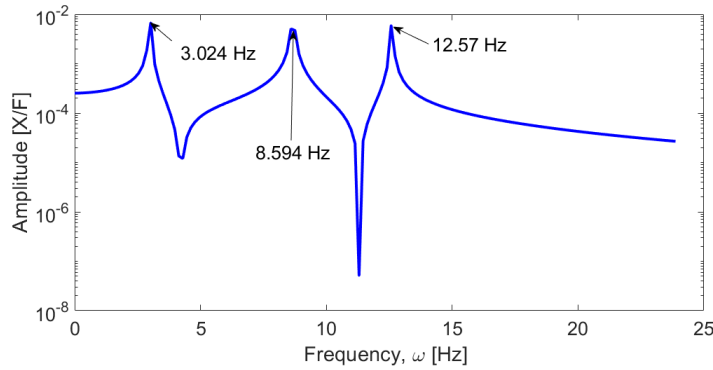


Fig. 4. Frequency response of the building model without absorber

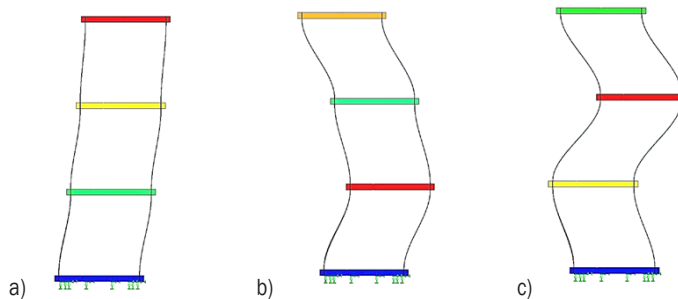


Fig. 5. a) Mode shape of the first resonant frequency, b) mode shape of the second resonant frequency, and c) mode shape of the third resonant frequency

amplitude is given in-floor displacement per unit force of excitation.

The simulation results show that with proper tuning of the electromagnetic stiffness, the AEMVA can effectively be used to reduce the vibration response of the structure.

4 EXPERIMENTAL SETUP

An experimental setup used to implement the AEMVA is shown in Fig 7. An accelerometer is attached to the third floor of the building model to measure the acceleration signal resulting from the vibration. This acceleration signal is used to construct the fast Fourier transform (FFT) diagrams and used to construct the amplitude-time signal for any time-domain analysis required.

An exciter consisting of a motor and an unbalance disk is mounted on the first floor of the building to exert the force needed to excite the building. The plate used for the first floor had a thickness of 5 mm to account for the weight of the exciter. A speed controller was used to adjust the motor’s rotating frequency. The absorber was mounted atop the building, and power supplies used were connected to the electromagnets for the current variation as required. The polarity

for each electromagnet was adjusted so the two electromagnets facing each other repel.

A Dewesoft Sirius Modular data acquisition system and software were used to acquire and process the accelerometer signals. The whole setup was mounted on a heavy steel plate for proper structure grounding, as in Fig. 7.

5 EXPERIMENTAL RESULTS

The effect of attaching AEMVA to the structure at the three resonant frequencies after adjusting the magnetic field to provide the necessary stiffness is shown in Fig. 8. The frequency response function of the building model is shown in Fig. 9. The current supplied to each electromagnet for each mode is shown in Table 3.

Table 3. Theoretical and experimental resonance and current combinations

Modes	Theoretical resonant frequency ω_n [Hz]	Experimental resonant frequencies ω_n [Hz]	Current supplied [A]
First	3.024	2.42	1.80
Second	8.754	7.66	2.60
Third	12.570	12.10	3.00

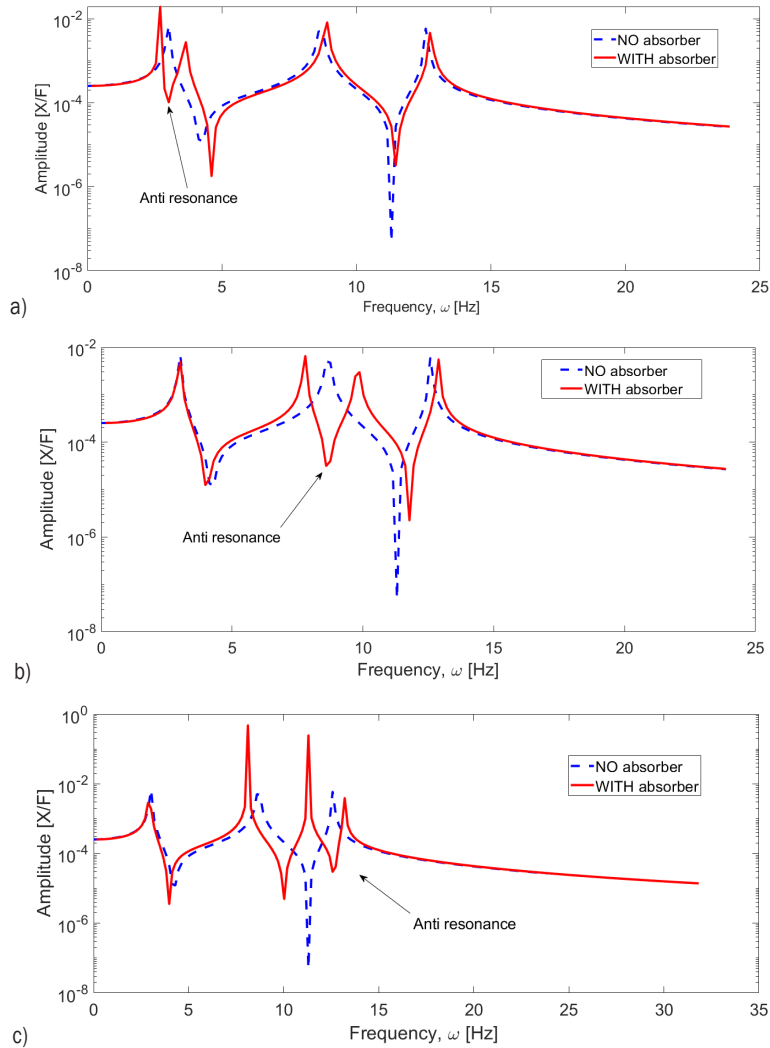


Fig. 6. a) Anti-resonance of the first mode, b) anti-resonance of the second mode, and c) anti-resonance of the third mode

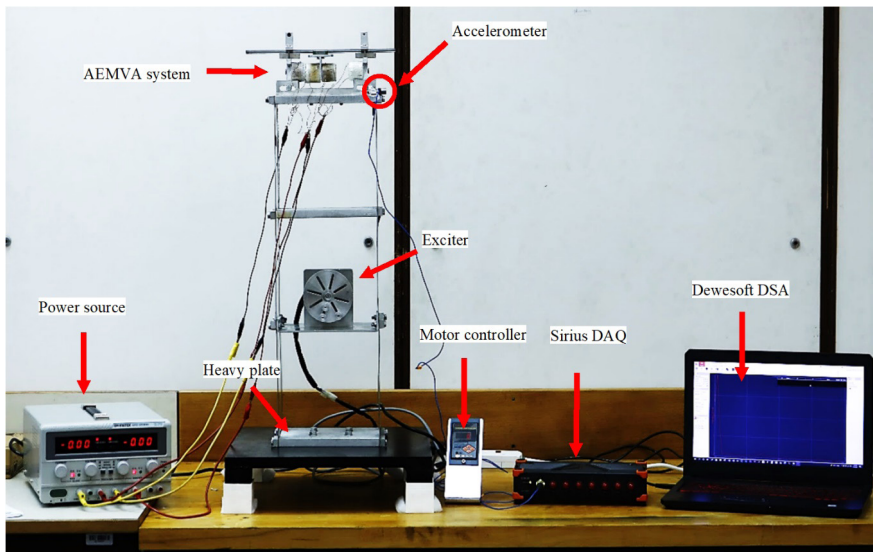


Fig. 7. Experimental setup

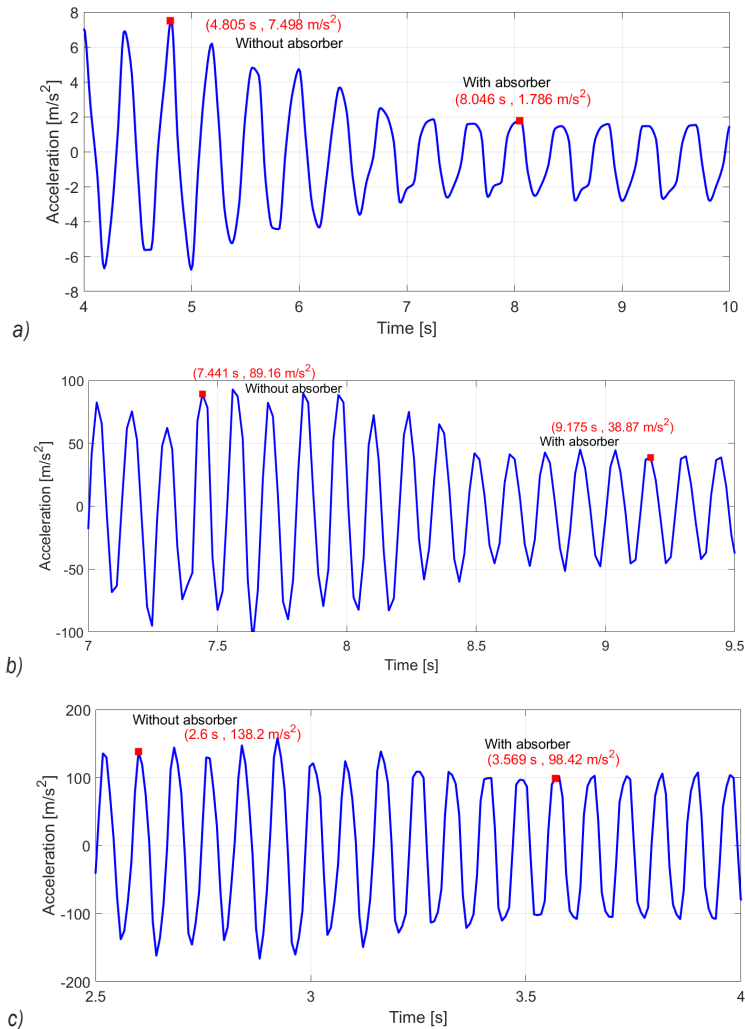


Fig. 8. a) Performance of AEMVA at first mode with and without the absorber, b) Performance of AEMVA at second mode with and without the absorber, and c) Performance of AEMVA at third mode with and without the absorber

Based on the summarized data in Table 4, Figs. 8 and 9, it is observed that the AEMVA successfully absorbs all three vibration modes. Three resonance frequencies at 2.42 Hz, 7.66 Hz, and 12.1 Hz had an amplitude attenuation of 68.81 %, 50.49 %, and 33.45 %, respectively. Notably, the third mode of frequency had a lower attenuation than the other two modes. This is due to the rapid vibration that resulted in the absorber colliding with the side electromagnets due to the small distance between them. The performance of the AEMVA at the third mode can be improved by increasing the current supplied to each electromagnet while increasing the distance between the electromagnets. This will result in a smoother oscillation without any collision but will cause excessive heating on electromagnets. The

general trend is that reducing the distance between the two electromagnets or increasing the current increases the stiffness coefficient. However, the distance cannot be minimal for any effective oscillation to occur; thus, experimenting with the current-distance combination can prove effective.

6 CONCLUSION

This research used an AEMVA to reduce the vibrations on a three-story building prototype model. Both simulation and experimental studies are presented in this work. By tuning the AEMVA, it is shown that the vibrations of the building floors were reduced due to the variations of the magnetic flux/stiffness. The tuning of AEMVA was achieved by changing

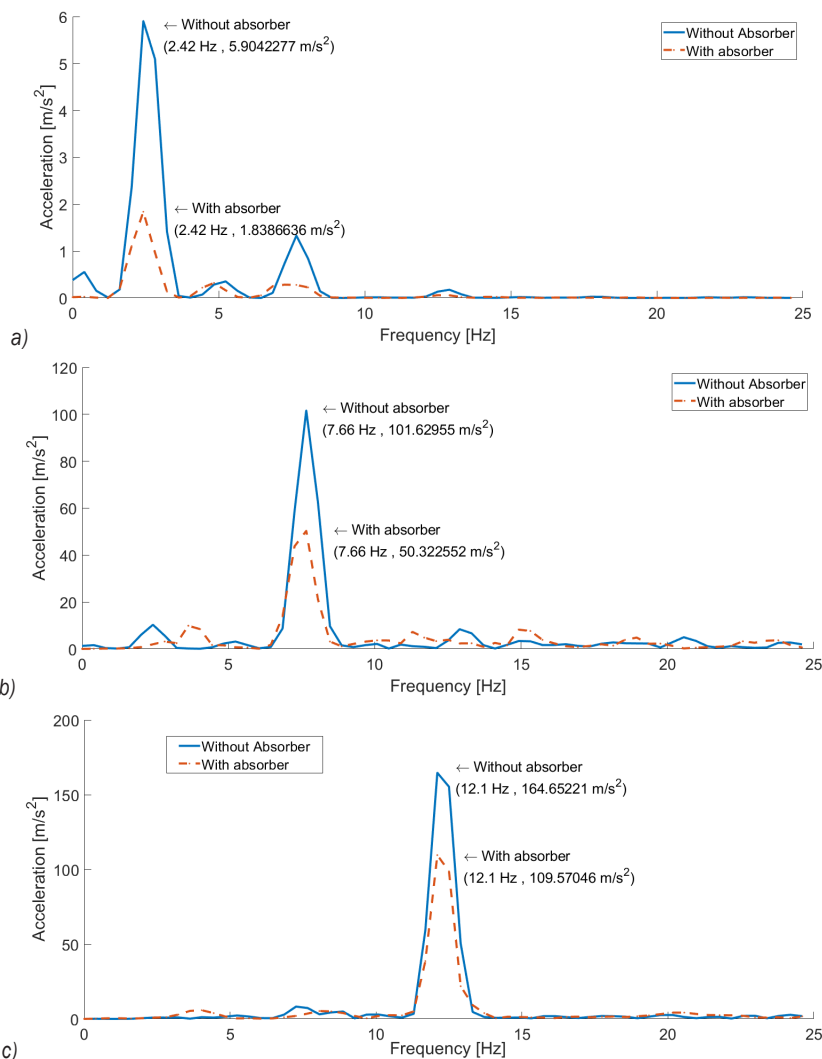


Fig. 9. a) Frequency response function at first mode, b) frequency response function at second mode, and c) frequency response function at second mode

Table 4. AEMVA performance at the resonant frequency

Modes	Resonant frequencies [Hz]	Vibration amplitude without AEMVA [m/s ²]	Vibration amplitude with AEMVA [m/s ²]	Attenuation amplitude [m/s ²]	Attenuation [%]
First	2.42	5.90	1.84	4.06	68.81
Second	7.66	101.63	50.32	51.31	50.49
Third	12.10	164.65	109.57	55.08	33.45

the current supply to each electromagnet to match the resonance frequencies of the model. Both simulation and experimental results show that a single absorber can suppress the effect of vibration at a multi-modal structure.

One point of interest is the slight shift in frequencies between the theoretical and experimental results and the attenuation, which was almost 100 % for all modes in the theoretical results. The frequency

shift is explained by how the theoretical results were conducted without accounting for the weight of the absorber on top of the structure and the weight of the excitation motor, which decreases the natural frequencies of the model. The difference in amplitude attenuation comes from the already assumed negligible damping. The constant collision of the absorber and side electromagnets also causes a lower-than-expected percentage attenuation. This was mostly observed in

the third mode of vibration, where the absorber's mass had a higher displacing force due to the rapid structure vibration.

7 ACKNOWLEDGEMENTS

This work is partly supported by Qatar University Student Grant no: QUST-2-CENG-2020-3.

8 REFERENCES

- [1] Hoang, T., Ducharme, K.T., Kim, Y., Okumus, P. (2016). Structural impact mitigation of bridge piers using tuned mass damper. *Engineering Structures*, vol. 112, p. 287-294, DOI:10.1016/j.engstruct.2015.12.041.
- [2] Bhattacharyya, S., Ghosh, A.D. Basu, B. (2017). Nonlinear modeling and validation of air spring effects in a sealed tuned liquid column damper for structural control. *Journal of Sound and Vibration*, vol. 410, p. 269-286, DOI:10.1016/j.jsv.2017.07.046.
- [3] Yuan, M., Sadhu, A., Liu, K. (2018). Condition assessment of structure with tuned mass damper using empirical wavelet transform. *Journal of Vibration and Control*, vol. 24, no. 20, p. 4850-4867, DOI:10.1177/1077546317736433.
- [4] Pandey, D.K., Sharma, M.K., Mishra, S.K. (2019). A compliant tuned liquid damper for controlling seismic vibration of short period structures. *Mechanical Systems and Signal Processing*, vol. 132, p. 405-428, DOI:10.1016/j.ymsp.2019.07.002.
- [5] Dai, J., Xu, Z.D., Gai, P.P. (2019). Tuned mass-damper-inerter control of wind-induced vibration of flexible structures based on inerter location. *Engineering Structures*, vol. 199, art. ID 109585, DOI:10.1016/j.engstruct.2019.109585.
- [6] Lee, C.Y., Pai, C.A. (2016). Design and implementation of tunable multi-degree-of-freedom vibration absorber made of hybrid shape memory helical springs. *Journal of Intelligent Material Systems and Structures*, vol. 27, no. 8, p. 1047-1060, DOI:10.1177/1045389X15581519.
- [7] Gao, N., Jeon, J.S., Hodgson, D.E., DesRoches, R. (2016). An innovative seismic bracing system based on a superelastic shape memory alloy ring. *Smart Materials and Structures*, vol. 25, no. 5, art. ID 055030, DOI:10.1088/0964-1726/25/5/055030.
- [8] Huang, H., Chang, W.S. (2020). Re-tuning an off-tuned tuned mass damper by adjusting temperature of shape memory alloy: Exposed to wind action. *Structures*, vol. 25, p. 180-189, DOI:10.1016/j.istruc.2020.02.025.
- [9] Ghasemi, M.R., Shabakhty, N., Enferadi, M.H. (2019). Vibration control of offshore jacket platforms through shape memory alloy pounding tuned mass damper (SMA-PTMD). *Ocean Engineering*, vol. 191, art. ID 106348, DOI:10.1016/j.oceaneng.2019.106348.
- [10] Yang, J., Sun, S., Tian, T., Li, W., Du, H., Alici, G., Nakano, M. (2016). Development of a novel multi-layer MRE isolator for suppression of building vibrations under seismic events. *Mechanical Systems and Signal Processing*, vol. 70, p. 811-820, DOI:10.1016/j.ymsp.2015.08.022.
- [11] Liao, G., Xu, Y., Wei, F., Ge, R., Wan, Q. (2017). Investigation on the phase-based fuzzy logic controller for magnetorheological elastomer vibration absorber. *Journal of Intelligent Material Systems and Structures*, vol. 28, no. 6, p. 728-739, DOI:10.1177/1045389X16657417.
- [12] Wang, Q., Dong, X., Li, L., Ou, J. (2017). Study on an improved variable stiffness tuned mass damper based on conical magnetorheological elastomer isolators. *Smart Materials and Structures*, vol. 26, no. 10, art. ID 105028, DOI:10.1088/1361-665X/aa81e8.
- [13] Ünker, F., Çuvalcı, O. (2019). Optimum tuning of a gyroscopic vibration absorber for vibration control of a vertical cantilever beam with tip mass. *International Journal of Acoustics & Vibration*, vol. 24, no. 2, p. 210-216, DOI:10.20855/ijav.2019.24.21158.
- [14] Zulkefli, A.M., Muthalif, A.G.A., Nordin, N.H.D., Syam, T.M. (2019). Intelligent glove for suppression of resting tremor in Parkinson's disease. *Vibroengineering PROCEDIA*, vol. 29, p. 176-181, DOI:10.21595/vp.2019.21078.
- [15] Davis, C.L., Lesieutre, G.A. (2000). An actively tuned solid-state vibration absorber using capacitive shunting of piezoelectric stiffness. *Journal of Sound and Vibration*, vol. 232, no. 3, p. 601-617, DOI:10.1006/jsvi.1999.2755.
- [16] Elmali, H., Renzulli, M., Olgac, N. (2000). Experimental comparison of delayed resonator and PD controlled vibration absorbers using electromagnetic actuators. *Journal of Dynamic Systems, Measurement, and Control*, vol. 122, no. 3, p. 514-520, DOI:10.1115/1.1286820.
- [17] McDaid, A.J. Mace, B.R. (2013). A self-tuning electromagnetic vibration absorber with adaptive shunt electronics. *Smart Materials and Structures*, vol. 22, no. 10, art. ID 105013, DOI:10.1088/0964-1726/22/10/105013.
- [18] Truong, D.Q., Ahn, K.K. (2012). MR fluid damper and its application to force sensorless damping control system. *Smart Actuation and Sensing Systems - Recent Advances and Future Challenges*, DOI:10.5772/51391.
- [19] Xu, Z.-D., Guo, Y.-Q. (2006). Fuzzy control method for earthquake mitigation structures with magnetorheological dampers. *Journal of Intelligent Material Systems and Structures*, vol. 17, no. 10, p. 871-881, DOI:10.1177/1045389X06061044.
- [20] Xu, Z.-D., Shen, Y.-P., Guo, Y.-Q. (2003). Semi-active control of Structures Incorporated with magnetorheological dampers using neural networks. *Smart Materials and Structures*, vol. 12, no. 1, p. 80-87, DOI:10.1088/0964-1726/12/1/309.
- [21] Xu, Z.-D., Shen, Y.-P. (2003). Intelligent bi-state control for the structure with magnetorheological dampers. *Journal of Intelligent Material Systems and Structures*, vol. 14, no. 1, p. 35-42, DOI:10.1177/1045389X03014001004.
- [22] Gonzalez-Buelga, A., Clare, L., Neild, S., Burrow, S., Inman, D. (2015). An electromagnetic vibration absorber with harvesting and tuning capabilities. *Structural Control and Health Monitoring*, vol. 22, no. 11, p. 1359-1372, DOI:10.1002/stc.1748.
- [23] Young, H.D., Freedman, R.A., Ford, A.L., Sears, F.W. (2014). 28.5 Magnetic Field of a Circular Current Loop. *Sears and Zemansky's University Physics: With Modern Physics*, p. 932-935, Pearson Education, San Francisco.